

Regular article

Thrombin-induced delayed injury involves multiple and distinct signaling pathways in the cerebral cortex and the striatum in organotypic slice cultures

Shinji Fujimoto, Hiroshi Katsuki, Toshiaki Kume, Akinori Akaike

Department of Pharmacology, Graduate School of Pharmaceutical Sciences, Kyoto University, 46-29 Yoshida-shimoadachi-cho, Sakyo-ku, Kyoto 606-8501, Japan.

Address correspondence to Akinori Akaike, Ph.D.

Department of Pharmacology,

Graduate School of Pharmaceutical Sciences, Kyoto University

46-29 Yoshida-shimoadachi-cho, Sakyo-ku, Kyoto 606-8501, Japan.

Phone: +81-75-753-4550 FAX: +81-75-753-4579

E-mail: aakaike@pharm.kyoto-u.ac.jp

Abstract

Thrombin, a serine protease essential for blood coagulation, also plays an important role in cellular injury associated with intracerebral hemorrhage. Here we show that, in organotypic cortico-striatal slice cultures, thrombin evoked delayed neuronal injury in the cerebral cortex and shrinkage of the striatum. These effects were prevented by cycloheximide and actinomycin D but not by a caspase-3 inhibitor. Thrombin-induced shrinkage of the striatum was abolished by a thrombin inhibitor argatroban or prior heat inactivation of thrombin, and significantly attenuated by a protease-activated receptor-1 antagonist FR171113. However, thrombin-induced cortical injury was not prevented either by heat inactivation or by FR171113, and was only partially inhibited by argatroban. In addition, inhibition of extracellular signal-regulated kinase (ERK), Src tyrosine kinase and protein kinase C prevented both neuronal injury in the cortex and shrinkage of the striatum, whereas inhibition of p38 mitogen-activated protein kinase and c-Jun *N*-terminal kinase prevented shrinkage of the striatum only. Thrombin treatment promptly induced phosphorylation of ERK, which was not prevented by inhibition of Src and protein kinase C. Thus, thrombin induces cellular injury in the cerebral cortex and the striatum, by recruiting multiple and distinct signaling pathways in protease activity-independent as well as dependent manner.

Keywords: apoptosis; intracerebral hemorrhage; mitogen-activated protein kinase; neurodegeneration; oxidative stress; thrombin

Introduction

Thrombin, a serine protease generated from prothrombin at sites of vascular injury, plays an important role in blood coagulation and wound healing. Prothrombin mRNA is also expressed in various brain regions (Dihanich et al., 1991), which indicates that thrombin may play a role as a signaling molecule in the central nervous system. Indeed, members of protease-activated receptor (PAR) family that mediate biological actions of thrombin are distributed widely throughout the central nervous system. Thrombin cleaves amino terminal exodomain of PAR-1, -3 and -4, and the newly generated amino terminus binds to the extracellular domain of the receptor as a tethered ligand (Noobakhsh et al., 2003). PARs are G protein-coupled receptors with seven transmembrane segments. Activation of these receptors leads to various kinds of intracellular signal transduction, including increase of intracellular calcium (Smith-Swintosky et al., 1995), decrease of cyclic AMP (Yang et al., 1997) and activation of protein kinase C (PKC) (Wang et al., 2002). In addition, several lines of evidence suggest that mitogen-activated protein kinases (MAPKs) are involved in thrombin-induced cellular responses (Marinissen et al., 2003; Suo et al., 2003; Wang et al., 2002).

At low concentrations, thrombin may provide cytoprotective effects on neurons and astrocytes against oxidative stress and ischemic injury (Donovan and Cunningham, 1998; Striggow et al., 2000; Vaughan et al., 1995). By contrast, uncontrolled thrombin activity after intracerebral hemorrhage results in gliosis and neural cell death. For example, experimental evidence *in vitro* has shown that thrombin causes neurite retraction in differentiated neural cell lines (Jalink and Moolenaar, 1992), and cell death in dissociated neuron cultures and cultured hippocampal slices (Donovan et al., 1997; Striggow et al., 2000; Suo et al., 2003). Intrastratial injection of thrombin causes neuronal degeneration *in vivo* (Xue et al., 2001), and neuronal injury and neurological dysfunction associated with

intracerebral hemorrhage are ameliorated by argatroban, a thrombin inhibitor (Kitaoka et al., 2002). Moreover, thrombin may also play a pivotal role in other pathological conditions including ischemic stroke, traumatic injury and Alzheimer's disease (Xi et al., 2003; Christov et al., 2004).

Despite these lines of evidence, little information is available concerning signaling mechanisms mediating cytotoxic actions of thrombin. Thrombin-induced neuronal death exhibits features of apoptosis (Donovan et al., 1997; Smirnova et al., 1998; Turgeon et al., 1998), and caspase inhibitors attenuate thrombin-induced cell death (Choi et al., 2003a; Turgeon et al., 1998). Activation of extracellular signal-regulated kinase (ERK), a kind of MAPKs, appears to be involved in thrombin-induced cell death in primary hippocampal neuron cultures (Suo et al., 2003). On the other hand, in the midbrain substantia nigra, thrombin induces degeneration of dopaminergic neurons indirectly via activation of microglia, which may involve several members of MAPK family such as ERK, p38 MAPK and c-Jun *N*-terminal kinase (JNK) (Choi et al., 2003a, 2003b; Lee et al., 2005). Contribution of multiple signaling mechanisms may differ among different experimental conditions and cellular contexts.

Intracerebral hemorrhage occur preferentially in several brain regions including the cerebral cortex and the striatum, but the detailed mechanisms of thrombin-induced injury in these brain regions remain to be determined. In this study, we investigated cytotoxic consequences of thrombin application to organotypic cortico-striatal slice cultures.

Materials and methods

Drugs and chemicals

Drugs and chemicals were obtained from Nacalai Tesque (Kyoto, Japan), unless otherwise indicated. Thrombin from bovine plasma (catalog No. T4648) was obtained from Sigma (St. Louis, MO, USA). Three different lots (022K7604, 061K7612 and 023K7602) of thrombin gave similar results. Bovine serum albumin (catalog No. A2153), MK-801, aminoguanidine, *N*^ω-nitro-L-arginine methyl ester (L-NAME), *N*-acetylcysteine (NAC) and clodronate were also obtained from Sigma. Cell-permeable DEVD-CHO, PD98059, U0126, SB203580, bisindolylmaleimide (BIM), 4-amino-5-(4-chlorophenyl)-7-(*t*-butyl)pyrazolo[3,4-*d*]pyrimidine (PP2) and 2-cyano-(3,4-dihydroxy)-*N*-benzylcinnamide (AG490) were obtained from Calbiochem (San Diego, CA, USA). SP600125 were obtained from Tocris Cookson (Bristol, UK). Cycloheximide and glutathione were obtained from Wako Pure Chemicals (Osaka, Japan). Argatroban was obtained from Sawai Pharmaceuticals (Osaka, Japan). FR171113 was a kind gift from Fujisawa Pharmaceuticals (Osaka, Japan).

Preparation of slice cultures

All experimental procedures were approved by our institutional animal experimentation committee, and animals were treated in accordance with the guidelines of the NIH regarding the care and use of animals for experimental procedures. We prepared organotypic slice cultures according to the methods described previously (Fujimoto et al., 2004). Briefly, Wistar rats at postnatal days 3 - 4 (Nihon SLC, Shizuoka, Japan) were anesthetized by hypothermia, brains were removed from the skull and separated into two hemispheres. Each hemisphere was cut into coronal slices of 300 μm thickness under sterile conditions. Slices containing the parietal cortex and the striatum were chosen, and other brain structures such as

the septum and the basal forebrain were removed from each slice. Six cortico-striatal tissue slices were transferred onto a 30-mm Millicell-CM insert membrane (Millipore, Bedford, MA, USA) in six-well plates. Culture medium, consisting of 50% minimum essential medium/HEPES (GIBCO, Invitrogen Japan, Tokyo, Japan), 25% Hanks' balanced salt solution (GIBCO) and 25% heat-inactivated horse serum (GIBCO) supplemented with 6.5 mg/ml D-glucose and 2 mM L-glutamine, 100 U/ml penicillin G potassium and 100 µg/ml streptomycin sulfate (GIBCO), was supplied at 0.75 ml/well so that the slices were maintained at liquid/air interface. Culture medium was exchanged for fresh one on the next day of culture preparation, and thereafter, every two days. Slices were cultured in a humidified atmosphere of 5% CO₂ and 95% air at 34°C.

Drug treatment and cell death assessment

Cultured slices at 9 - 11 days *in vitro* were incubated for 24 - 48 h in serum-free medium, where minimum essential medium/HEPES substituted for horse serum. Then slices were exposed to thrombin and other drugs dissolved in serum-free medium for indicated periods. To assess cell injury, propidium iodide (PI; 5 µg/ml) was added to serum-free medium for drug treatment. After indicated periods, PI fluorescence of each slice was observed with an inverted fluorescence microscope with a rhodamine filter set and a 10× objective lens. Fluorescence images were captured through a monochrome chilled CCD camera (C5985; Hamamatsu Photonics, Hamamatsu, Japan) and stored as image files. The intensity of each pixel was expressed as an 8-bit signal (0 - 255), and the average signal intensity in an area of 180 µm × 180 µm within the parietal cortex was obtained as the fluorescence value of each slice, with the use of NIH Image 1.63 software. In each experiment, slice cultures treated with 100 µM *N*-methyl-D-aspartate (NMDA) for 72 h were used to determine the degree of the standard injury. Fluorescence values were normalized with the intensity of cultures that

received standard injury as 100%. Images of whole slice cultures were also obtained through a 1× objective lens, and the area of the striatal region in each slice was estimated with NIH Image 1.63.

Immunohistochemistry and nuclear staining

After drug treatment, slice cultures were fixed with 0.1 M phosphate buffer containing 4% paraformaldehyde and 4% sucrose for 2 h. After rinse with phosphate-buffered saline (PBS), they were permeabilized and blocked by 0.1% Triton X-100 in PBS containing 1.5 % horse serum or goat serum, then incubated with primary antibodies overnight at 4°C. Primary antibodies were mouse anti-NeuN (1:200, Chemicon International, Temecula, CA, USA), mouse anti-OX42 (1:300, Dainippon Pharmaceutical, Osaka, Japan), mouse anti-glia fibrillary acidic protein (GFAP) (1:500, Sigma), and rabbit anti-phospho-p44/42 MAP kinase (T202/Y204) (1:250, Cell Signaling Technology, Beverly, MA, USA). After rinse with PBS, cultures were incubated with secondary antibodies for 1 h at room temperature. Alexa Fluor 568-labeled goat anti-rabbit IgG (1:1000, Molecular Probes, Eugene, OR, USA), Alexa Fluor 488-labeled goat anti-mouse IgG (1:1000, Molecular Probes), Alexa Fluor 568-labeled goat anti-mouse IgG (1:1000, Molecular Probes), Cy2-conjugated goat anti-rabbit IgG (1:1600, Jackson Immunoresearch Laboratories, West Grove, PA, USA) and Cy3-conjugated goat anti-mouse IgG (1:1600, Jackson Immunoresearch Laboratories) were used as secondary antibodies. In several experiments, Alexa Fluor 488-conjugated isolectin GS-IB4 from *Griffonia simplicifolia* (1 µg/ml, Molecular Probes) was added to the secondary antibody solution. Then cultures were rinsed with PBS and specimens were dehydrated through a graded series of ethanol and mounted on slide glasses with glycerol. Fluorescence signals were observed with a laser-scanning confocal microscopic system (MRC1024, Biorad, Hercules, CA, USA).

In several experiments, cell nuclei were stained with Hoechst 33342 (Molecular Probes). Cultures fixed with 4% paraformaldehyde as mentioned above were incubated with 0.1 mg/ml Hoechst 33342 for 60 min. After wash with PBS, fluorescence images were acquired through an upright epifluorescence microscope.

Nitrite quantification

Amount of nitric oxide released during treatment with thrombin was quantified as a concentration of nitrite in culture medium (Shibata et al., 2003). Culture supernatants (100 μ l) were subjected to a reaction with an equal volume of Griess reagent (1% sulfanilamide and 0.1% *N*-(1-naphthyl)-ethylenediamine dihydrochloride in 2.5% phosphoric acid) for 10 min at room temperature. Absorbance of diazonium compound was measured at 540 nm on a microplate reader. Absolute levels of nitrite were determined with reference to a standard curve obtained from defined concentrations of sodium nitrite.

Western blot analysis

After treatment with thrombin and drugs for indicated periods, slice cultures were harvested and homogenized in ice-cold lysis buffer containing 20 mM Tris-HCl (pH 7.0), 25 mM β -glycerophosphate (Sigma), 2 mM EGTA-2Na, 1% Triton X-100, 1 mM vanadate, 1% aprotinin (Sigma), 1 mM phenylmethylsulfonyl fluoride and 2 mM dithiothreitol. Samples were mixed with a sample buffer composed of 124 mM Tris-HCl (pH 6.8), 4% sodium dodecyl sulfate (SDS), 10% glycerol, 0.02% bromophenol blue and 4% 2-mercaptoethanol. After boiling for 5 min, samples were subjected to 12% SDS-polyacrylamide gel electrophoresis for 70 min, followed by transfer to PVDF membrane (Millipore) for 70 min. Membranes were blocked for at least 1 h by 5% nonfat milk at room temperature and subsequently incubated overnight with mouse anti-phospho-p44/42 MAP kinase (T202/Y204)

(1:2000, Cell Signaling Technology), anti-p44/42 MAP kinase (1:1000, Cell Signaling Technology) and goat anti- β -actin (1:3000, Santa Cruz Biotechnology, Santa Cruz, CA, USA). The membranes were rinsed and incubated with horseradish peroxidase-conjugated goat anti-mouse IgG (1:10000, Jackson Immunoresearch Laboratories), goat anti-rabbit IgG (1:10000, Jackson Immunoresearch Laboratories) and horse anti-goat IgG (1:10000, Vector Laboratories, Burlingame, CA, USA). After incubation with secondary antibodies, membranes were rinsed and bound antibodies were detected with enhanced chemiluminescence kit (Amersham Biosciences, Buckinghamshire, UK) according to the manufacturer's instructions. The band intensities were analyzed with NIH image 1.63.

Statistics

Data are expressed as means \pm S.E.M. Statistical significance of difference was evaluated with one-way analysis of variance followed by Student–Newman–Keuls' test. Probability values less than 5% were considered significant.

Results

Thrombin induces delayed cortical neuron death and striatal degeneration

Cortico-striatal slices were maintained for 9 - 11 days in culture. As previously described (Fujimoto et al., 2004), the striatal region gradually flattened during cultivation and typically left monolayer of cells, whereas the cortical region maintained much thicker appearance than the striatal region. These cultures were exposed to thrombin at concentrations of 10 - 300 U/ml for 72 h, and PI fluorescence was used as a measure of cell injury. We could also observe the entire morphology of individual slices probed by faint background fluorescence of PI (Fig. 1A-L).

Thrombin induced two prominent changes in cortico-striatal slice cultures. First, in the cortical region, we observed a drastic increase in PI fluorescence indicating cell death. The cytotoxic effect of thrombin in the cortex was evident at concentrations of 100 and 300 U/ml. Cell death occurred in a delayed manner: thrombin at 100 U/ml did not show cytotoxic effect at 24 h, and a robust increase in PI fluorescence was observed at 72 h after the onset of thrombin exposure (Fig. 1Q). Second, shrinkage of the tissue was observed in a delayed manner. Particularly, the area of the striatal region displayed a marked decrease in response to treatment with 100 and 300 U/ml thrombin for 48 - 72 h. A lower concentration (30 U/ml) of thrombin also caused a significant decrease in the striatal area after 72 h of treatment (Fig. 1R). The shrinkage seemed to be initiated by focal detachment of the tissue, concomitantly with cell death around the corresponding area (Fig. 1M, N). We did not determine which cell types underwent cell death in this area, because detached tissue was difficult to be examined immunohistochemically, and also because tissue detachment *per se* was likely to induce cell death that may obscure the conclusion. The rest of the striatal region that remained attached to the membrane contained viable neurons, astrocytes and microglia (data not shown), which did not support the possibility that selective loss of a

particular type of cells in the striatal region accounts for the shrinkage. In contrast, we never observed shrinkage of cortico-striatal tissues after treatment with NMDA (Fig. 1O, P).

Striatal injury after NMDA application observed by macroscopic PI fluorescence (Fig. 1P) was not so clear as cortical injury, because the striatal region consisted of much thinner layer of cells than the cortical region, and also because some populations of the striatal neurons were resistant to NMDA cytotoxicity. We confirmed by close examination that PI-positive cells appeared in the striatal region after NMDA treatment. Bovine serum albumin, at a protein concentration corresponding to that of 100 U/ml of thrombin, did not show any cytotoxic effects on the cortical and the striatal regions (data not shown).

To identify cell types that caused cell death in the cortical region in response to thrombin, we performed immunohistochemical examinations using antibodies against cell type-specific marker proteins such as NeuN (a neuronal marker), OX42 (a microglial marker) and GFAP (an astrocyte marker). We found that numerous NeuN-positive cells were present in the cortical region of slice cultures without thrombin treatment, whereas application of thrombin to the cultures for 72 h caused a marked decrease in the number of immunoreactive cells (Fig. 2A, B). We also performed NeuN immunohistochemistry on slices after uptake of PI, according to the method of Brana et al. (2002). We observed co-localization of PI fluorescence and NeuN immunoreactivity, which indicated that these dying cells were neurons. Several PI-positive cells were not stained or were only weakly stained by NeuN, which may be in part due to loss of immunoreactivity during progression of degeneration processes (arrows in Fig. 2B). Interestingly, double fluorescence examinations revealed that a significant population of OX42-positive microglia also contained PI fluorescence (Fig. 2D). After thrombin treatment, the number of OX42-immunoreactive cells did not decrease, but the morphology of these cells changed from resting ramified form into activated amoeboid form (Fig. 2C, D). Therefore, co-localization of PI fluorescence and OX42 immunoreactivity

might reflect phagocytic activity of activated microglia on dying neurons. To examine this possibility, we utilized fluorophore-labeled isolectin GS-IB4 to identify microglia and compared the pattern of isolectin staining with that of NeuN immunoreactivity. No isolectin-positive cells engulfed NeuN-positive cells at 48 - 72 h after thrombin exposure (Fig. 2G, H), indicating that PI- and OX42-positive cells (Fig. 2D) represent dying microglia rather than microglia incorporating dying neurons. In contrast to these observations, no co-localization of PI fluorescence with GFAP immunoreactivity was apparent (Fig. 2E, F). These results suggest that the dying cell population in the cortical region of slice cultures after thrombin treatment consists mainly of neurons and also includes microglia.

Thrombin cytotoxicity exhibits several features of apoptosis but is independent of caspase-3

Several studies reported that thrombin induces apoptosis of neuronal as well as non-neuronal cells (Donovan et al., 1997), and that caspase inhibitors block thrombin cytotoxicity (Smirnova et al., 1998; Turgeon et al., 1998). Accordingly, we examined if apoptotic processes are involved in thrombin toxicity in cortico-striatal slice cultures. First, morphological changes in cell nuclei after thrombin treatment were examined by nuclear staining with Hoechst 33342. As shown in Fig. 3A, nuclei of cells bearing diffuse staining with the Hoechst dye exhibited round or oval morphology in untreated slice cultures. In contrast, a number of condensed and fragmented nuclei appeared in slices treated with 100 U/ml thrombin for 72 h (Fig. 3B). Second, we examined if macromolecule synthesis was required for thrombin cytotoxicity. Concomitant application of cycloheximide (1 µg/ml), a protein synthesis inhibitor, with thrombin abolished cell death in the cortical region (Fig. 3C). An mRNA synthesis inhibitor actinomycin D (1 µg/ml) produced a similar effect to that of cycloheximide, negating thrombin cytotoxicity in the cortical region almost completely (Fig. 3D). These drugs also reversed thrombin-induced shrinkage of the striatal region (Fig. 3F).

Third, we examined possible involvement of caspase-3, an executioner caspase involved in apoptotic cell death induced by various stimuli (Leist and Jäättelä, 2001). Concurrent application of cell-permeable DEVD-CHO, a caspase-3 inhibitor, did not produce any effects on thrombin-induced cell death in the cortical region and shrinkage of the striatal region (Fig. 3E, G). These results suggest that thrombin-induced injury requires *de novo* protein synthesis but not caspase-3 activity.

Differential involvement of protease activity and PAR-1 in thrombin toxicity in the cortex and in the striatum

We examined if protease activity of thrombin and activation of thrombin receptors were responsible for thrombin cytotoxicity. PARs, after removal of their amino-terminal domain by protease activity of thrombin, mediate various biological actions of thrombin (Noorbakhsh et al., 2003). However, thrombin may also exert some of its biological effects through protease activity- and/or PAR-independent mechanisms (Tran and Stewart, 2003; Hanisch et al., 2004).

We tested the effect of argatroban, a drug that inhibits enzymatic activity of thrombin by binding to the hydrophobic pocket (Kikumoto et al., 1984). We found that argatroban (30 - 300 μ M) significantly but only partially attenuated thrombin cytotoxicity in the cortical region (Fig. 4A). On the other hand, argatroban (300 μ M) completely blocked thrombin-induced shrinkage of the striatal region (Fig. 4D). Notably, prior heat inactivation of thrombin only weakly inhibited thrombin cytotoxicity at 48 h and had no effect at 72 h in the cortical region (Fig. 4C), whereas the same procedure abolished induction of shrinkage of the striatal region by thrombin (Fig. 4F). Moreover, we examined the effect of a PAR-1 antagonist FR171113 (Kato et al., 2003). FR171113 (300 μ M) did not inhibit thrombin-induced cell death in the cortical region (Fig. 4B), whereas the drug significantly

inhibited thrombin-induced shrinkage of the striatal region (Fig. 4E). These results suggest that cytotoxicity of thrombin in the striatum is dependent on the protease activity of thrombin and activation of PAR-1, whereas cytotoxicity of thrombin in the cerebral cortex involves protease activity-independent mechanisms.

In hippocampal neurons, thrombin has been reported to potentiate NMDA receptor function via activation of PAR1 (Gingrich et al., 2000). To clarify if NMDA receptors are involved in thrombin toxicity, we examined the effect of MK-801. Co-application of 10 μ M MK-801 with 100 U/ml thrombin did not prevent either cortical injury or striatal shrinkage (data not shown).

MAPKs are differentially involved in thrombin toxicity in the cortex and in the striatum

Distinct classes of MAPKs such as ERK, p38 MAPK and JNK play important roles in regulation of neuronal survival and death (Colucci-D'Amato et al., 2003; Davis, 2000; Gallo and Johnson, 2002). Because several members of MAPK family have been reported to mediate various biological responses induced by thrombin (Möller et al., 2000; Suo et al., 2003; Wang et al., 2002), we examined the effects of MAPK inhibitors on thrombin cytotoxicity in cortico-striatal slice cultures. PD98059 (10 - 100 μ M) and U0126 (1 - 10 μ M), drugs that compromise ERK activation by inhibiting mitogen/extracellular signal-regulated kinase (MEK), significantly reduced thrombin-induced cell death in the cortical region (Fig. 5B, C, F, G). On the other hand, SB203580 (10 - 100 μ M), an inhibitor of p38 MAPK, did not inhibit thrombin cytotoxicity in the cortical region (Fig. 5D, H). The cytotoxicity of SB203580 *per se*, as evident in Fig. 5D, was not consistently observed in the other sets of experiments. Notably, SP600125 (10 - 100 μ M), a JNK inhibitor, strongly potentiated thrombin cytotoxicity in the cortex (Fig. 5E, I). However, all of these inhibitors of MAPK pathways markedly attenuated thrombin-induced shrinkage of the striatal region (Fig.

5J). These results indicate that ERK is involved in thrombin-induced neuronal death in the cortex, whereas ERK, p38 and JNK are involved in thrombin-induced shrinkage of the striatum.

Involvement of microglia in thrombin cytotoxicity

We further examined potential involvement of other signal mediators in thrombin cytotoxicity. In the midbrain substantia nigra, thrombin toxicity on dopaminergic neurons appears to be mediated by microglia producing cytotoxic mediators including nitric oxide (NO) (Choi et al., 2003a). In addition, a recent report showed that thrombin-induced damage in the hippocampus was mediated by reactive oxygen species produced from microglia (Choi et al., 2005). Accordingly, we tested the effects of NO synthase inhibitors and antioxidants on thrombin cytotoxicity. We indeed found that cytotoxic concentrations (100 - 300 U/ml) of thrombin increased NO production from cortico-striatal slice cultures at 48 - 72 h (Fig. 6A, B). The increase in NO production was almost completely blocked by NO synthase inhibitors aminoguanidine and L-NAME, each at 300 μ M (data not shown). However, these inhibitors did not produce significant protective effects against thrombin-induced cell death in the cortical region (Fig. 6C for the data on L-NAME) and shrinkage of the striatal region (Fig. 6D). Moreover, antioxidants glutathione (data not shown) and NAC (Fig. 6E, F) were also without effect against thrombin toxicity in the cortex and in the striatum. Activated microglia may also produce potentially cytotoxic factors other than NO and reactive oxygen species. Therefore, we collected conditioned medium of slice cultures treated with 100 U/ml thrombin for 72 h, and treated another set of slice cultures with the conditioned medium. The potency of cytotoxicity of the conditioned medium was the same as that of fresh culture medium containing 100 U/ml thrombin (data not shown). These results do not support the proposal that diffusible cytotoxic factors are released in

response to thrombin.

Next we examined the effect of clodronate, a drug shown to deplete microglia from brain slice cultures (Kohl et al., 2003). We confirmed that slice cultures treated with clodronate (100 $\mu\text{g/ml}$) and thrombin had much fewer microglia than cultures treated with thrombin alone (Fig. 6G, H). In addition, cultures treated with clodronate and thrombin produced a smaller amount of nitrite than cultures treated with thrombin alone ($11.7 \pm 1.0 \mu\text{M}$, $n = 3$ and $32.8 \pm 5.0 \mu\text{M}$, $n = 4$, with or without clodronate, respectively; $P < 0.01$). However, clodronate did not affect the degree of thrombin-induced injury in the cortical region (Fig. 6I). These results suggest that microglial activation does not contribute to cortical injury by thrombin. Interestingly, thrombin-induced shrinkage of the striatal region was significantly inhibited by clodronate treatment (Fig. 6J).

Thrombin cytotoxicity is regulated by Src and protein kinase C

Thrombin-induced activation of ERK in cultured astrocytes is regulated by several upstream signaling molecules including Src protein tyrosine kinase and PKC (Wang et al., 2002; Wang and Reiser, 2003). Considering that ERK activation plays a key role in thrombin cytotoxicity (Fig. 5), we examined possible involvement of Src and PKC. Concurrent application of PP2 (10-100 μM), an inhibitor of Src, with thrombin reduced cell injury in the cortical region in a concentration-dependent manner (Fig. 7A, B, D). In contrast, AG490, an inhibitor of JAK2 protein tyrosine kinase, did not show any protective effect at concentrations up to 100 μM (data not shown). We also found that BIM (0.3 - 3 μM), an inhibitor of PKC, prevented thrombin-induced cell injury in the cortical region (Fig. 7C, E). PP2 and BIM were also effective in inhibiting thrombin-induced shrinkage of the striatal region (Fig. 7F). Together, these results suggest that Src and PKC contribute to thrombin cytotoxicity.

Thrombin induces rapid ERK phosphorylation independently of Src and protein kinase C

We next examined the time course of ERK phosphorylation in response to thrombin by western blot analysis. Levels of phosphorylated ERK increased promptly after thrombin application, peaked at 1 - 3 h and gradually declined thereafter (Fig. 8A, B). To determine cell types exhibiting ERK phosphorylation after 3 h of thrombin treatment, we performed double immunofluorescence staining with a combination of antibodies against phosphorylated ERK and cell type-specific marker proteins. Immunostaining with the neuronal marker NeuN revealed that many of the phospho-ERK-positive cells were neurons (Fig. 8C-E). We could not determine whether these phospho-ERK-positive neurons corresponded to ultimately dying cells, because ERK phosphorylation declined before cell death became prominent. We also observed co-localization of phospho-ERK with the microglia marker OX42 (Fig. 8F) and with the astrocyte marker GFAP (Fig. 8G). However, the glial population positive for phospho-ERK was much smaller than phospho-ERK-positive neuronal population.

We examined the effects of inhibitors of Src and PKC on thrombin-induced ERK phosphorylation, to determine if these signaling molecules act upstream of ERK activation. As expected, the MEK inhibitor PD98059 (100 μ M) abolished thrombin-induced increase in ERK phosphorylation. In sharp contrast, the Src inhibitor PP2 at 100 μ M, a concentration that significantly reduced thrombin cytotoxicity (Fig. 7), showed no effect on thrombin-induced ERK phosphorylation. In addition, the PKC inhibitor BIM (3 μ M) did not inhibit, but rather, potentiated ERK phosphorylation (Fig. 8H, I). These results indicate that thrombin induces ERK phosphorylation in Src- and PKC-independent manner, and also that Src and PKC regulate thrombin cytotoxicity independently of ERK regulation.

Although ERK was phosphorylated promptly after thrombin exposure, cell injury in the cortical region and shrinkage of the striatal region occurred with a long delay (see Fig. 1).

Therefore, we examined whether these detrimental effects could be triggered by a shorter period of thrombin exposure. Exposure of the cultures to thrombin for 24 h followed by incubation in thrombin-free medium did not induce significant cell death in the cortical region. Robust cell death was induced when the period of thrombin application was extended to 36 h or longer (Fig. 9A). Shrinkage of the striatal region was induced by 24 h exposure to thrombin followed by 48 h of post-incubation in thrombin-free medium. However, longer periods of exposure such as 48 h were required for thrombin to fully exert the detrimental effect (Fig. 9B). These results suggest that persistent signaling, in addition to rapid ERK phosphorylation, is required for induction of cell death by thrombin.

Discussion

Accumulating evidence indicates that thrombin exerts deleterious effects in the central nervous system under several pathological conditions including intracerebral hemorrhage (Gingrich and Traynelis, 2000; Xi et al., 2003). Because thrombin receptors are expressed not only in neurons but also in astrocytes and microglia (Grabham and Cunnigham, 1995; Suo et al., 2002), thrombin extravasation should mobilize complicated processes that lead to cellular injury. In this study we used organotypic cortico-striatal slice cultures to evaluate cytotoxicity of thrombin, and found that prolonged application of thrombin produces cytotoxic effects with a delayed onset. Thrombin showed robust cytotoxic actions at 100 U/ml. This is a concentration attainable in the case of hemorrhagic injury, because prothrombin in 100 μ l of blood is estimated to produce ~30 U thrombin (Xi et al., 2003). Histochemical examinations revealed that dying cells in the cortical region of slice cultures after thrombin treatment consisted mainly of neurons and also included some microglia but not astrocytes, although thrombin causes cell death in astrocytes as well as neurons in dissociated cell culture preparations (Donovan et al., 1997). In addition to robust cell death in the cortical region, thrombin caused shrinkage of the cultured tissue, particularly in the striatal region. The striatal shrinkage is a unique feature of thrombin cytotoxicity, because we have not observed shrinkage of the tissues in response to other cytotoxic insults we tested so far, including NMDA and oxygen-glucose deprivation (Fujimoto et al., 2004).

Apoptotic cell death is accompanied by morphological changes in cell nuclei such as condensation and fragmentation. In addition, macromolecule synthesis is required for many, if not all, cases of apoptotic cell death (Holcik and Sonenberg, 2005). Previous reports have demonstrated that thrombin induces nuclear fragmentation, and cycloheximide prevents thrombin-induced cell death in cultured hippocampal neurons (Donovan et al., 1997). In line with these observations, we observed that numerous cells in the cortical region exhibited

nuclear fragmentation in response to thrombin, and also that cycloheximide and actinomycin D prevented thrombin toxicity in the cortex and in the striatum. On the other hand, a caspase-3 inhibitor did not inhibit thrombin cytotoxicity, although the involvement of this executioner caspase in thrombin-induced apoptosis has been suggested in cultured motor neurons (Turgeon et al., 1998) and in midbrain dopaminergic neurons *in vivo* (Choi et al., 2003a). In this context, apoptosis-like cell death in the absence of caspase activation has been documented (Leist and Jäättelä, 2001; Sperandio et al., 2000). A recent report showed that ERK activation led to nuclear condensation and cell death of rat cerebellar granule neurons, which was independent of caspase-3 (Subramaniam et al., 2004).

Although thrombin induced delayed injury both in the cerebral cortex and in the striatum, underlying mechanisms of thrombin cytotoxicity were different between these brain regions. In the striatal region, the actions of thrombin are likely to be mediated by its protease activity and activation of PAR-1, since thrombin-induced shrinkage of the striatal region was abolished by argatroban as well as by heat inactivation of thrombin, and was significantly inhibited by a PAR-1 antagonist. In contrast, argatroban only partially inhibited thrombin-induced cortical cell death, and heat inactivation of thrombin and co-application of a PAR-1 antagonist were without effect. Protease activity-independent action of thrombin has been reported in the case of microglial activation (Hanisch et al., 2004). Moreover, PAR-independent actions of thrombin have been reported in airway smooth muscle cells (Tran and Stewart, 2003). How thrombin can exert biological actions independently of its protease activity is unclear, but thrombin may somehow activate several signaling pathways including ERK, Src and PKC, as discussed below.

We showed here that ERK activation plays an important role in thrombin cytotoxicity, based on the observation that inhibition of ERK phosphorylation by MEK inhibitors significantly attenuated thrombin-induced cell death in the cortical region and shrinkage of

the striatal region. Protective effect of MEK inhibitors against thrombin cytotoxicity has been previously demonstrated in cultured hippocampal cell line (Suo et al., 2003) and in midbrain dopaminergic neurons *in vivo* (Choi et al., 2003a). We additionally found that inhibition of p38 did not affect, whereas inhibition of JNK exacerbated, thrombin-induced cortical cell death. Generally, JNK activation is linked to apoptotic cell death induced by various stimuli including nerve growth factor deprivation (Ham et al., 1995) and excitatory amino acids (Borsello et al., 2003), but neuroprotection by JNK activation through the mechanisms involving astrocyte-derived diffusible factors have also been reported (Dhandapani et al., 2003). Elucidation of detailed regulatory mechanisms of thrombin cytotoxicity by JNK requires further investigation. What is more interesting is that inhibitors of MEK, p38 and JNK all attenuated thrombin-induced shrinkage of the striatal region, which indicates that multiple members of MAPK family are involved in striatal degeneration induced by thrombin. These results also suggest that thrombin recruits different signaling mechanisms leading to cellular injury in different brain regions.

Thrombin can activate microglia (Ryu et al., 2000; Suo et al., 2002), and microglial activation may constitute an important aspect of thrombin-induced degeneration of midbrain dopaminergic neurons (Choi et al., 2003a) and hippocampal neurons (Choi et al., 2005) *in vivo*. In addition, microglia-induced neuronal injury may be mediated by production of NO and reactive oxygen species (Choi et al., 2003a, 2005). However, we did not observe significant protective effect of NO synthase inhibitors and antioxidants against thrombin-induced injury in the cerebral cortex and in the striatum. Moreover, depletion of microglia by clodronate did not prevent thrombin cytotoxicity in the cortical region. Therefore, in the cortical region, thrombin is likely to produce cytotoxic effects by directly acting on neurons, rather than by indirectly acting through microglial activation, although the contribution of glial cells to neuronal degeneration cannot be entirely excluded. The fact

that the majority of phospho-ERK-positive cells after thrombin treatment were neurons is also consistent with this proposal. In contrast, thrombin toxicity in the striatal region was significantly inhibited by clodronate. These observations reveal another difference between the cerebral cortex and the striatum with respect to thrombin-induced injury.

Src and PKC were shown to act upstream of ERK phosphorylation in thrombin signaling pathway leading to proliferation of astrocytes (Wang et al., 2002; Wang and Reiser, 2003) and oligodendrocytes (Lin et al., 2005). Based on the assumption that ERK phosphorylation leading to thrombin-induced cell death might also be regulated by Src and PKC, we examined potential involvement of these signaling molecules in thrombin cytotoxicity. We found that inhibitors of Src and PKC significantly prevented thrombin-induced cell injury. Unexpectedly, however, these inhibitors did not prevent thrombin-induced ERK phosphorylation. Therefore, Src and PKC are involved in the signaling cascade leading to neuronal death, independently of regulation of ERK activation. In this context, protein tyrosine kinase-independent ERK phosphorylation in response to thrombin has been hypothesized in platelets (Tulasne et al., 2002).

Involvement of signaling pathways other than ERKs in thrombin cytotoxicity was also suggested by comparison of the time course of ERK phosphorylation with the period of application required for thrombin cytotoxicity. ERK phosphorylation was promptly induced by thrombin application, peaked at 1 - 3 h and then declined gradually, whereas prolonged treatment (36 h or more) was required for full development of cell death by thrombin. Therefore, ERK activation *per se* may be unable to trigger cell injury, and other persistent signaling mechanisms are also essential for thrombin cytotoxicity. Whether Src and/or PKC correspond to this persistent signaling remains to be determined.

In this study, we revealed that complex signaling mechanisms underlie the cytotoxic actions of thrombin in cortico-striatal tissues. Cytotoxic signaling recruited by thrombin

appears to be different between different brain regions, but we also showed here that ERK activation mediates thrombin cytotoxicity both in the cortex and in the striatum. ERK activation occurs during the early phase of thrombin exposure, which leads to delayed neuronal death displaying several apoptosis-like features. Elucidation of the detailed mechanisms of thrombin signaling during induction of neuronal death, in particular the downstream targets of ERKs, may present a novel strategy of therapeutic interventions against intracerebral hemorrhage and other neuropathological conditions.

Acknowledgements

This study was supported by Grant-in-aid for Scientific Research from The Ministry of Education, Culture, Sports, Science and Technology, Japan, and Japan Society for the Promotion of Science.

References

- Borsello, T., Clarke, P.G., Hirt, L., Vercelli, A., Repici, M., Schorderet, D.F., Bogousslavsky, J., Bonny, C., 2003. A peptide inhibitor of c-Jun N-terminal kinase protects against excitotoxicity and cerebral ischemia. *Nat. Med.* 9, 1180-1186.
- Brana, C., Benham, C., Sundstrom, L., 2002. A method for characterising cell death in vitro by combining propidium iodide staining with immunohistochemistry. *Brain Res. Protoc.* 10, 109-114.
- Choi, S.-H., Joe, E.H., Kim, S.U., Jin, B.K., 2003a. Thrombin-induced microglial activation produces degeneration of nigral dopaminergic neurons in vivo. *J. Neurosci.* 23, 5877-5886.
- Choi, S.-H., Lee, D.Y., Ryu, J.K., Kim, J., Joe, E.H., Jin, B.K., 2003b. Thrombin induces nigral dopaminergic neurodegeneration in vivo by altering expression of death-related proteins. *Neurobiol. Dis.* 14, 181-193.
- Choi, S.-H., Lee, D.Y., Kim, S.U., Jin, B.K., 2005. Thrombin-induced oxidative stress contributes to the death of hippocampal neurons *in vivo*: role of microglial NADPH oxidase. *J. Neurosci.* 25, 4082-4090.
- Christov, A., Ottman, J.T., Grammas, P., 2004. Vascular inflammatory, oxidative and protease-based processes: implications for neuronal cell death in Alzheimer's disease. *Neurol. Res.* 26, 540-546.
- Colucci-D'Amato, L., Perrone-Capano, C., di Porzio, U., 2003. Chronic activation of ERK and neurodegenerative diseases. *Bioessays* 25, 1085-1095.
- Davis, R.J., 2000. Signal transduction by the JNK group of MAP kinases. *Cell* 103, 239-252.
- Dhandapani, K.M., Hadman, M., De Sevilla, L., Wade, M.F., Mahesh, V.B., Brann, D.W., 2003. Astrocyte protection of neurons: role of transforming growth factor-beta signaling via a c-Jun-AP-1 protective pathway. *J. Biol. Chem.* 278, 43329-43339.

- Dihanich, M., Kaser, M., Reinhard, E., Cunningham, D., Monard, D., 1991. Prothrombin mRNA is expressed by cells of the nervous system. *Neuron* 6, 575-581.
- Donovan, F.M., Pike, C.J., Cotman, C.W., Cunningham, D.D., 1997. Thrombin induces apoptosis in cultured neurons and astrocytes via a pathway requiring tyrosine kinase and RhoA activities. *J. Neurosci.* 17, 5316-5326.
- Donovan, F.M., Cunningham, D.D., 1998. Signaling pathways involved in thrombin-induced cell protection. *J. Biol. Chem.* 273, 12746-12752.
- Fujimoto, S., Katsuki, H., Kume, T., Kaneko, S., Akaike, A., 2004. Mechanisms of oxygen glucose deprivation-induced glutamate release from cerebrocortical slice cultures. *Neurosci. Res.* 50, 179-187.
- Gallo, K.A., Johnson, G.L., 2002. Mixed-lineage kinase control of JNK and p38 MAPK pathways. *Nat. Rev. Mol. Cell Biol.* 3, 663-672.
- Gingrich, M.B., Traynelis, S.F., 2000. Serine proteases and brain damage - is there a link? *Trends Neurosci.* 23, 399-407.
- Gingrich, M.B., Junge, C.E., Lyuboslavsky, P., Traynelis, S.F., 2000. Potentiation of NMDA receptor function by the serine protease thrombin. *J. Neurosci.* 20, 4582-4595.
- Grabham, P., Cunningham, D.D., 1995. Thrombin receptor activation stimulates astrocyte proliferation and reversal of stellation by distinct pathways: involvement of tyrosine phosphorylation. *J. Neurochem.* 64, 583-591.
- Ham, J., Babij, C., Whitfield, J., Pfarr, C.M., Lallemand, D., Yaniv, M., Rubin, L.L., 1995. A c-Jun dominant negative mutant protects sympathetic neurons against programmed cell death. *Neuron* 14, 927-939.
- Hanisch, U.K., van Rossum, D., Xie, Y., Gast, K., Misselwitz, R., Auriola, S., Goldsteins, G., Koistinaho, J., Kettenmann, H., Möller, T., 2004. The microglia-activating potential of thrombin: the protease is not involved in the induction of proinflammatory cytokines and

- chemokines. *J. Biol. Chem.* 279, 51880-51887.
- Holcik, M., Sonenberg, N., 2005. Translational control in stress and apoptosis. *Nat. Rev. Mol. Cell Biol.* 6, 318-327.
- Jalink, K., Moolenaar, W.H., 1992. Thrombin receptor activation causes rapid neural cell rounding and neurite retraction independent of classic second messengers. *J. Cell Biol.* 118, 411-419.
- Kato, Y., Kita, Y., Hirasawa-Taniyama, Y., Nishio, M., Mihara, K., Ito, K., Yamanaka, T., Seki, J., Miyata, S., Mutoh, S., 2003. Inhibition of arterial thrombosis by a protease-activated receptor 1 antagonist, FR171113, in the guinea pig. *Eur. J. Pharmacol.* 473, 163-169.
- Kikumoto, R., Tamao, Y., Tezuka, T., Tonomura, S., Hara, H., Ninomiya, K., Hijikata, A., Okamoto, S., 1984. Selective inhibition of thrombin by (2R,4R)-4-methyl-1-[N²-[(3-methyl-1,2,3,4-tetrahydro-8-quinolinyl)sulfonyl]-L-arginyl]-2-piperidinecarboxylic acid. *Biochemistry* 23, 85-90.
- Kitaoka, T., Hua, Y., Xi, G., Hoff, J.T., Keep, R.F., 2002. Delayed argatroban treatment reduces edema in a rat model of intracerebral hemorrhage. *Stroke* 33, 3012-3018.
- Kohl, A., Dehghani, F., Korf, H.W., Hailer, N.P., 2003. The bisphosphonate clodronate depletes microglial cells in excitotoxically injured organotypic hippocampal slice cultures. *Exp. Neurol.* 181, 1-11.
- Lee, D.Y., Oh, Y.J., Jin, B.K., 2005. Thrombin-activated microglia contribute to death of dopaminergic neurons in rat mesencephalic cultures: Dual roles of mitogen-activated protein kinase signaling pathways. *Glia* 51, 98-110.
- Leist, M., Jäättelä, M., 2001. Four deaths and a funeral: from caspases to alternative mechanisms. *Nat. Rev. Mol. Cell Biol.* 2, 589-598.
- Lin, X., Ramamurthy, S.K., Le Breton, G.C., 2005. Thromboxane A₂ receptor-mediated cell proliferation, survival and gene expression in oligodendrocytes. *J. Neurochem.* 93,

257-268.

Marinissen, M.J., Servitja, J.M., Offermanns, S., Simon, M.I., Gutkind, J.S., 2003. Thrombin protease-activated receptor-1 signals through G_q- and G₁₃-initiated MAPK cascades regulating c-Jun expression to induce cell transformation. *J. Biol. Chem.* 278, 46814-46825.

Möller, T., Hanisch, U.K., Ransom, B.R., 2000. Thrombin-induced activation of cultured rodent microglia. *J. Neurochem.* 75, 1539-1547.

Noorbakhsh, F., Vergnolle, N., Hollenberg, M.D., Power, C., 2003. Proteinase-activated receptors in the nervous system. *Nat. Rev. Neurosci.* 4, 981-990.

Ryu, J., Pyo, H., Jou, I., Joe, E., 2000. Thrombin induces NO release from cultured rat microglia via protein kinase C, mitogen-activated protein kinase, and NF-kappa B. *J. Biol. Chem.* 275, 29955-29959.

Shibata, H., Katsuki, H., Nishiwaki, M., Kume, T., Kaneko, S., Akaike, A., 2003.

Lipopolysaccharide-induced dopaminergic cell death in rat midbrain slice cultures: role of inducible nitric oxide synthase and protection by indomethacin. *J. Neurochem.* 86, 1201-1212.

Smirnova, I.V., Zhang, S.X., Citron, B.A., Arnold, P.M., Festoff, B.W., 1998. Thrombin is an extracellular signal that activates intracellular death protease pathways inducing apoptosis in model motor neurons. *J. Neurobiol.* 36, 64-80.

Smith-Swintosky, V.L., Zimmer, S., Fenton, J.W. II, Mattson, M.P., 1995. Protease nexin-1 and thrombin modulate neuronal Ca²⁺ homeostasis and sensitivity to glucose deprivation-induced injury. *J. Neurosci.* 15, 5840-5850.

Sperandio, S., de Belle, I., Bredesen, D.E., 2000. An alternative, nonapoptotic form of programmed cell death. *Proc. Natl. Acad. Sci. USA.* 97, 14376-14381.

Strigrow, F., Riek, M., Breder, J., Henrich-Noack, P., Reymann, K.G., Reiser, G., 2000. The

protease thrombin is an endogenous mediator of hippocampal neuroprotection against ischemia at low concentrations but causes degeneration at high concentrations. *Proc. Natl. Acad. Sci. USA.* 97, 2264-2269.

Subramaniam, S., Zirrgiebel, U., von Bohlen und Halbach, O., Strelau, J., Laliberté, C., Kaplan, D.R., Unsicker, K., 2004. ERK activation promotes neuronal degeneration predominantly through plasma membrane damage and independently of caspase-3. *J. Cell Biol.* 165, 357-369.

Suo, Z., Wu, M., Ameenuddin, S., Anderson, H.E., Zoloty, J.E., Citron, B.A., Andrade-Gordon, P., Festoff, B.W., 2002. Participation of protease-activated receptor-1 in thrombin-induced microglial activation. *J. Neurochem.* 80, 655-666.

Suo, Z., Wu, M., Citron, B.A., Palazzo, R.E., Festoff, B.W., 2003. Rapid tau aggregation and delayed hippocampal neuronal death induced by persistent thrombin signaling. *J. Biol. Chem.* 278, 37681-37689.

Tran, T., Stewart, A.G., 2003. Protease-activated receptor (PAR)-independent growth and pro-inflammatory actions of thrombin on human cultured airway smooth muscle. *Br. J. Pharmacol.* 138, 865-875.

Tulasne, D., Bori, T., Watson, S.P., 2002. Regulation of RAS in human platelets. Evidence that activation of RAS is not sufficient to lead to ERK1-2 phosphorylation. *Eur. J. Biochem.* 269, 1511-1517.

Turgeon, V.L., Lloyd, E.D., Wang, S., Festoff, B.W., Houenou, L.J., 1998. Thrombin perturbs neurite outgrowth and induces apoptotic cell death in enriched chick spinal motoneuron cultures through caspase activation. *J. Neurosci.* 18, 6882-6891.

Vaughan, P.J., Pike, C.J., Cotman, C.W., Cunningham, D.D., 1995. Thrombin receptor activation protects neurons and astrocytes from cell death produced by environmental insults. *J. Neurosci.* 15, 5389-5401.

- Wang, H., Ubl, J.J., Stricker, R., Reiser, G., 2002. Thrombin (PAR-1)-induced proliferation in astrocytes via MAPK involves multiple signaling pathways. *Am. J. Physiol. Cell Physiol.* 283, C1351-1364.
- Wang, H., Reiser, G., 2003. The role of the Ca²⁺-sensitive tyrosine kinase Pyk2 and Src in thrombin signalling in rat astrocytes. *J. Neurochem.* 84, 1349-1357.
- Xi, G., Reiser, G., Keep, R.F., 2003. The role of thrombin and thrombin receptors in ischemic, hemorrhagic and traumatic brain injury: deleterious or protective? *J. Neurochem.* 84, 3-9.
- Xue, M., Del Bigio, M.R., 2001. Acute tissue damage after injections of thrombin and plasmin into rat striatum. *Stroke* 32, 2164-2169.
- Yang, Y., Akiyama, H., Fenton, J.W. II, Brewer, G.J., 1997. Thrombin receptor on rat primary hippocampal neurons: coupled calcium and cAMP responses. *Brain Res.* 761, 11-18.

Figure Legends

Fig. 1. Thrombin-induced cortical cell injury and striatal shrinkage. (A-L) Representative images of PI fluorescence of whole cultured slices exposed to vehicle (A, D, G, J), 100 U/ml thrombin (B, E, H, K) and 300 U/ml thrombin (C, F, I, L) for 0 h (before exposure), 24 h, 48 h and 72 h, respectively. Broken lines in panels A-C and J-L indicate areas of the cerebral cortex (Cx) and the striatum (St). Scale bar, 1 mm. (M) An image of PI fluorescence of another slice culture exposed to 100 U/ml thrombin for 72 h. (N) An image at a high magnification of the region indicated by the solid line in panel M. The asterisk (*) indicates the area of the striatal region detaching from the membrane. Scale bar, 200 μ m. (O, P) Representative images of PI fluorescence of whole cultured slices exposed to 100 μ M NMDA for 0 h (M) and 72 h (N). (Q) Thrombin-induced cortical cell injury as assessed by intensity of PI fluorescence. Thrombin at indicated concentrations were applied for indicated periods. ## $P < 0.01$, ### $P < 0.001$ vs. vehicle (veh) at respective time points ($n = 5-6$). (R) Thrombin-induced striatal shrinkage as assessed by measurement of the striatal area. Thrombin at indicated concentrations were applied for indicated periods. * $P < 0.05$, *** $P < 0.001$ vs. 0 h of respective treatment ($n = 12$).

Fig. 2. (A-F) Confocal images of the cortical region of slice cultures exposed to vehicle (A, C, E) and thrombin (100 U/ml) (B, D, F) for 72 h and immunostained for cell type-specific markers. PI fluorescence (red) was colocalized with Neu N and OX42 immunoreactivity (green, B, D), markers of neurons and microglia, respectively, but not with GFAP immunoreactivity (green, F), a marker of astrocytes. Arrowheads indicate colocalization of immunoreactivity with PI. Arrows in B indicate PI-positive and weakly Neu N-stained cells, reflecting progression of degeneration processes. (G, H) Fluorescence-labeled NeuN immunoreactivity (red) and fluorescence-labeled isolectin GS-IB4 (green) in the cortical

region of slice cultures exposed to 100 U/ml thrombin for 48 h (G) and 72 h (H). No engulfing activity of isolectin-positive microglia against neuronal nuclei was evident. Scale bar, 20 μ m.

Fig. 3. Thrombin-induced cell injury accompanies nuclear fragmentation, and is dependent on new protein synthesis but not on caspase activity. (A, B) Nuclear morphology in the cortical region as revealed by Hoechst 33342 staining, after treatment of slice cultures with vehicle (A) and 100 U/ml thrombin (B) for 72 h. Arrowheads indicate nuclear fragmentation. Scale bar, 50 μ m. (C-E) Effects of cycloheximide (CHX; C), actinomycin D (AD; D) and DEVD-CHO (DEVD; E) on thrombin-induced cell injury in the cortical region. Drugs at indicated concentrations were concomitantly applied with 100 U/ml thrombin, and cell death was assessed at 48 and 72 h. (F, G) Effects of CHX, AD (F) and DEVD (G) on thrombin (100 U/ml)-induced shrinkage of the striatal region at 72 h. # $P < 0.05$, ### $P < 0.001$ vs. vehicle, * $P < 0.05$, ** $P < 0.01$, *** $P < 0.001$ vs. thrombin alone.

Fig. 4. Involvement of protease activity and PAR-1 activation in thrombin cytotoxicity. (A-C) Effects of argatroban (A), FR171113 (B) and heat inactivation (C) on thrombin-induced cell injury in the cortical region. Argatroban at indicated concentrations was applied concomitantly with 100 U/ml thrombin. FR171113 was applied at indicated concentrations from 24 h before and during thrombin application. "H" indicates heat treatment of drug solution achieved by incubation in boiling water for 15 min. (D-F) Effects of argatroban (ARG, 300 μ M; D), FR171113 (FR, 300 μ M; E) and heat inactivation (F) on thrombin (100 U/ml)-induced shrinkage of the striatal region at 72 h. ## $P < 0.01$, ### $P < 0.001$ vs. vehicle, * $P < 0.05$, ** $P < 0.01$, *** $P < 0.001$ vs. thrombin alone.

Fig. 5. Differential involvement of MAPKs in thrombin toxicity in the cortex and in the striatum. (A-E) Representative images of PI fluorescence of whole cultured slices exposed for 72 h to 100 U/ml thrombin alone (A), thrombin plus PD98059 (100 μ M; B), U0126 (10 μ M; C), SB203580 (100 μ M; D) or SP600125 (100 μ M; E). Scale bar, 1 mm. (F-I) Effects of MAPK inhibitors on thrombin-induced cell injury in the cortical region. PD98059 (F), U0126 (G), SB203580 (H) and SP600125 (I) at indicated concentrations were concomitantly applied with 100 U/ml thrombin, and cell death was assessed at 48 and 72 h. (J) Effects of MAPK inhibitors at the highest concentration examined on thrombin (100 U/ml)-induced shrinkage of the striatal region at 72 h. # $P < 0.05$, ### $P < 0.001$ vs. vehicle, * $P < 0.05$, ** $P < 0.01$, *** $P < 0.001$ vs. thrombin alone.

Fig. 6. Involvement of nitric oxide production, oxidative stress and microglia activation in thrombin toxicity. (A, B) Concentration- and time-dependent accumulation of nitrite in culture medium in response to thrombin. In (A), nitrite levels were determined after 72 h of treatment with indicated concentrations of thrombin. In (B), nitrite levels were determined after indicated periods of treatment with 100 U/ml thrombin. (C) Effects of L-NAME on cell injury in the cortical region. L-NAME at indicated concentrations was concomitantly applied with 100 U/ml thrombin, and cell death was assessed at 48 and 72 h. (D) Effects of aminoguanidine (AG, 300 μ M) and L-NAME (300 μ M) on thrombin (100 U/ml)-induced shrinkage of the striatal region at 72 h. (E) Effect of NAC on thrombin-induced cell injury in the cortical region. NAC at indicated concentrations was concomitantly applied with 100 U/ml thrombin, and cell death was assessed at 48 and 72 h. (F) Effects of NAC (1 mM) on thrombin-induced shrinkage of the striatal region at 72 h. (G-J) Effect of clodronate on microglia population and thrombin toxicity. Clodronate was applied to slice cultures from 72 h before and during treatment with vehicle or thrombin. Slice cultures exposed to

thrombin for 72 h in the absence (G) or presence (H) of clodronate (100 $\mu\text{g}/\text{ml}$) were immunostained for OX42, a marker of microglia. Scale bar, 50 μm . Clodronate (10 – 100 $\mu\text{g}/\text{ml}$) did not protect the cortical region from thrombin-induced injury (I), but striatal shrinkage was prevented by 100 $\mu\text{g}/\text{ml}$ clodronate (CLO; J). ## $P < 0.01$, ### $P < 0.001$ vs. vehicle, *** $P < 0.001$ vs. thrombin alone.

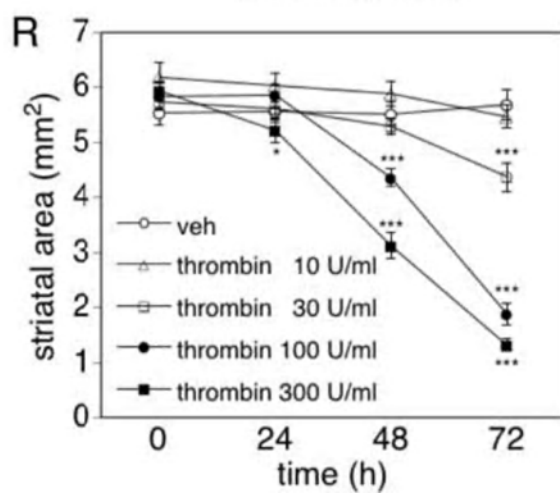
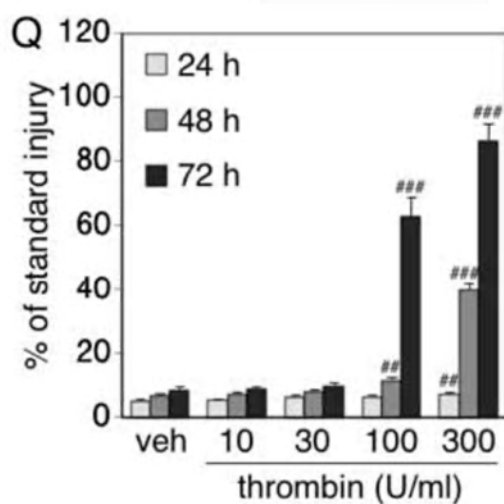
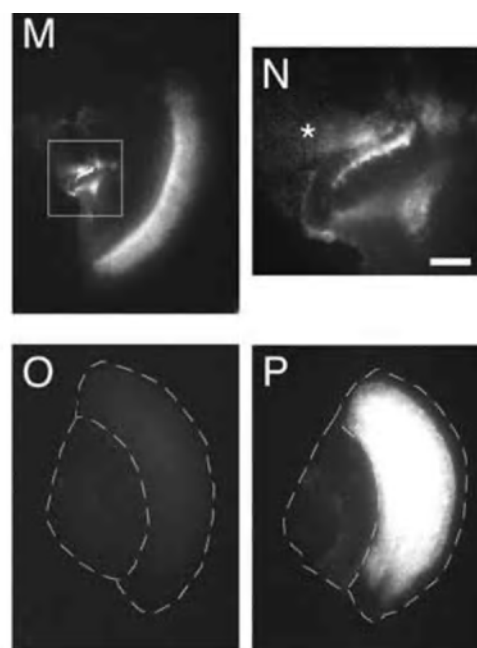
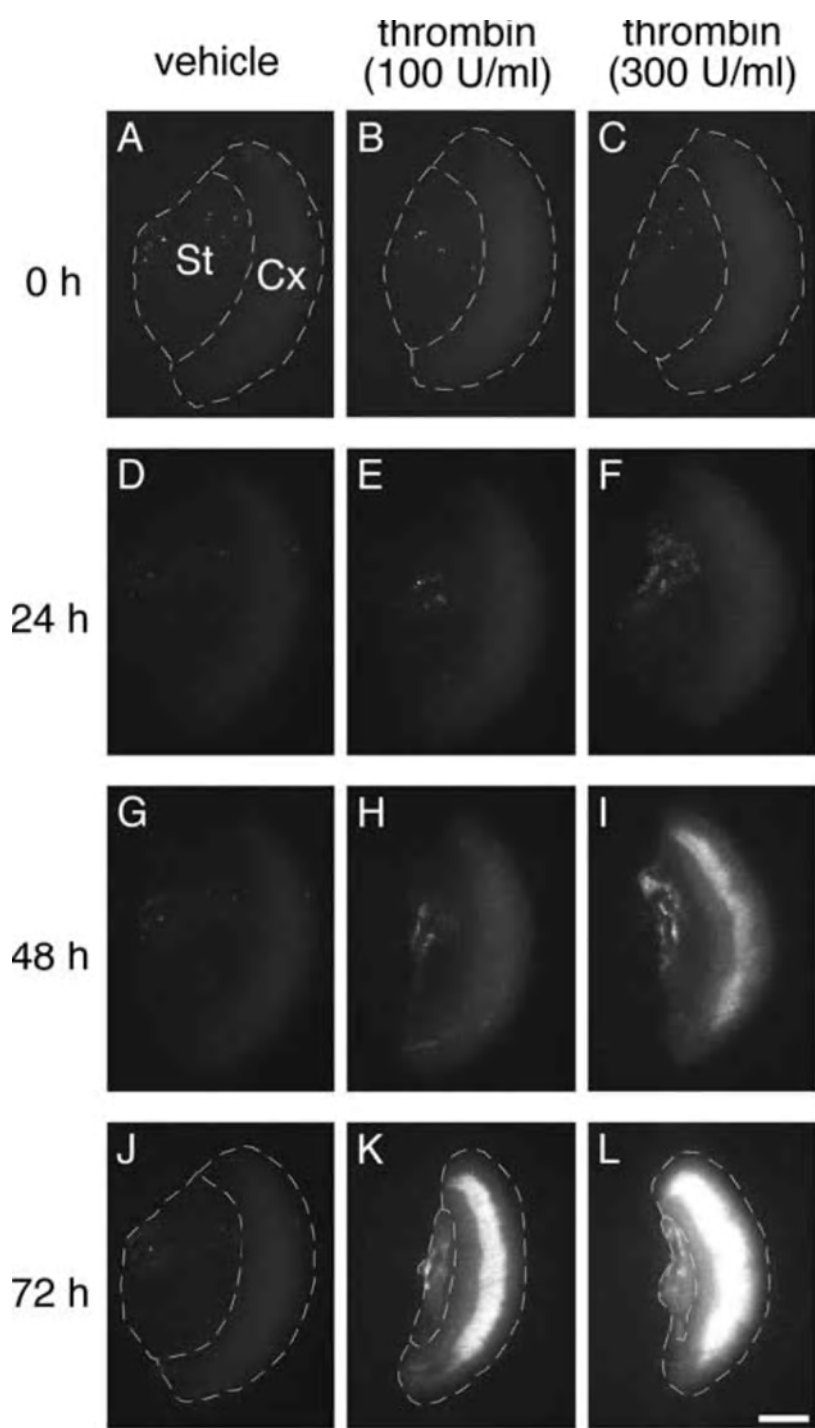
Fig. 7. Effects of inhibitors of Src and PKC on thrombin cytotoxicity. (A-C)

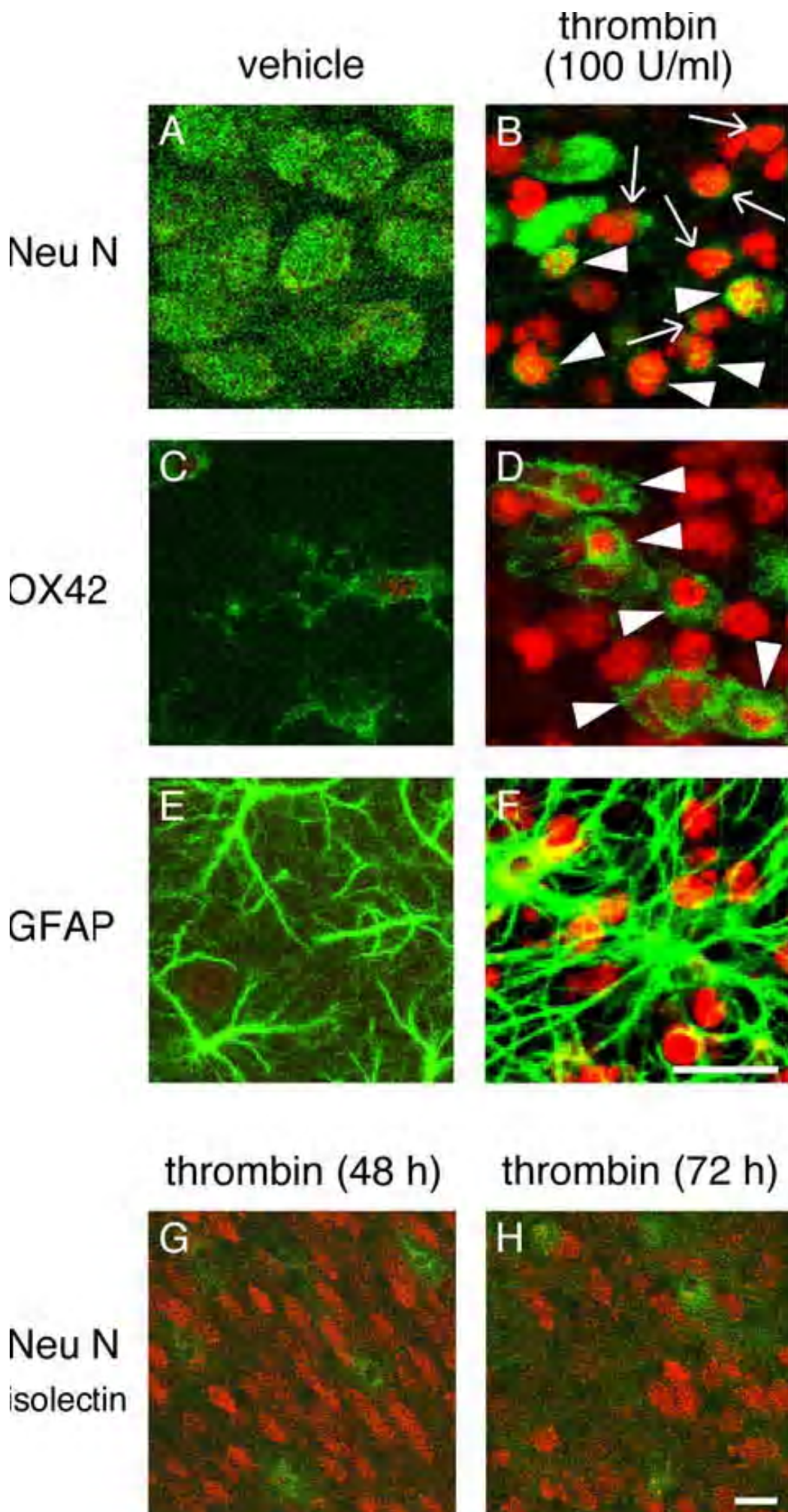
Representative images of PI fluorescence of whole cultured slices exposed to 100 U/ml thrombin alone (A), and thrombin plus PP2 (100 μM ; B) or BIM (3 μM ; C) for 72 h. Scale bar, 1 mm. (D, E) Effects of inhibitors of Src and PKC on thrombin-induced cell injury in the cortical region. PP2 (D) and BIM (E) at indicated concentrations were concomitantly applied with 100 U/ml thrombin, and cell death was assessed at 48 and 72 h. (F) Effects of inhibitors of Src and PKC at the highest concentration examined on thrombin (100 U/ml)-induced shrinkage of the striatal region at 72 h. ## $P < 0.01$, ### $P < 0.001$ vs. vehicle, * $P < 0.05$, ** $P < 0.01$, *** $P < 0.001$ vs. thrombin alone.

Fig. 8. Thrombin-induced phosphorylation of ERKs. (A) Representative blots of ERK phosphorylation in response to thrombin. Homogenates were prepared from whole slice cultures treated with thrombin (100 U/ml) for indicated periods and lysates were subjected to western blot analysis with specific antibodies against phosphorylated ERK, total ERK and actin. Slices without thrombin treatment (0 h) were used as control. (B) Time course of ERK phosphorylation. Ratio of phospho-ERK versus total ERK at each time point was normalized by the ratio at time 0. # $P < 0.05$, ## $P < 0.01$, ### $P < 0.001$ vs. time 0 (n = 5). (C-G) Confocal microscopic images of immunofluorescence of phospho-ERK (C), Neu N (D) and their merged image (E), and merged images of phospho-ERK (green) and OX42 (red, F)

or GFAP (red, G), after 3 h of treatment with 100 U/ml thrombin. Arrowheads indicate co-localization. Scale bar, 20 μm . (H) Representative blots showing the effects of drugs on thrombin-induced ERK phosphorylation. Western blot analysis was performed on slice cultures that received no treatment (NT), vehicle treatment (V), 100 U/ml thrombin with or without PD98059 (PD; 100 μM), PP2 (100 μM) and BIM (3 μM) for 3 h. (I) Summary of the effects of drugs on ERK phosphorylation. # $P < 0.05$ vs. no treatment, * $P < 0.05$ vs. thrombin alone ($n = 4$).

Fig. 9. Persistent signaling is required for induction of cell death by thrombin. Slice cultures were treated with 100 U/ml thrombin for hours indicated on the left side of slash (/) and subsequently incubated without thrombin for hours indicated on the right side of slash. Cell injury in the cortical region (A) and shrinkage of the striatal region (B) were assessed at 72 h after the onset of treatments. ### $P < 0.001$ vs. vehicle (indicated as "0/72").





vehicle

thrombin (100 U/ml)

